BJP British Journal of Pharmacology

DOI:10.1111/bph.12999
www.brjpharmacol.org

RESEARCH PAPER

Novel Nrf2 activators from microbial transformation products inhibit blood–retinal barrier permeability in rabbits

Yasuhiro Nakagami[1], Kayoko Masuda[2], Emiko Hatano[1], Tatsuya Inoue[1], Takuya Matsuyama[1], Mayumi Iizuka[2], Yasunori Ono[2], Takashi Ohnuki[2], Yoko Murakami[2], Masaru Iwasaki[2], Kazuhiro Yoshida[1], Yuji Kasuya[1] and Satoshi Komoriya[1]

[1]*Daiichi Sankyo Co., Ltd., Tokyo, Japan, and* [2]*Daiichi Sankyo RD Novare Co., Ltd., Tokyo, Japan*

Correspondence
Yasuhiro Nakagami, Daiichi Sankyo Co., Ltd., 1-2-58, Hiromachi, Shinagawa-ku, Tokyo 140-8710, Japan. E-mail: nakagami.yasuhiro.y4@daiichisankyo.co.jp

Received
17 July 2014
Revised
20 October 2014
Accepted
24 October 2014

BACKGROUND AND PURPOSE

Nuclear factor erythroid 2-related factor 2 (Nrf2) is a redox-sensitive transcription factor that binds to antioxidant response elements located in the promoter region of genes encoding many antioxidant enzymes and phase II detoxifying enzymes. Activation of the Nrf2 pathway seems protective for many organs, and although a well-known Nrf2 activator, bardoxolone methyl, was evaluated clinically for treating chronic kidney disease, it was found to induce adverse events. Many bardoxolone methyl derivatives, mostly derived by chemical modifications, have already been studied. However, we adopted a biotransformation technique to obtain a novel Nrf2 activator.

EXPERIMENTAL APPROACH

The potent novel Nrf2 activator, RS9, was obtained from microbial transformation products. Its Nrf2 activity was evaluated by determining NADPH:quinone oxidoreductase-1 induction activity in Hepa1c1c7 cells. We also investigated the effects of RS9 on oxygen-induced retinopathy in rats and glycated albumin-induced blood–retinal barrier permeability in rabbits because many ocular diseases are associated with oxidative stress and inflammation.

KEY RESULTS

Bardoxolone methyl doubled the specific activity of Nrf2 in Hepa1c1c7 cells at a much higher concentration than RS9. Moreover, the induction of Nrf2-targeted genes was observed at a one-tenth lower concentration of RS9. Interestingly, the cytotoxicity of RS9 was substantially reduced compared with bardoxolone methyl. Oral and intravitreal administration of RS9 ameliorated the pathological scores and leakage in the models of retinopathy in rats and ocular inflammation in rabbits respectively.

CONCLUSION AND IMPLICATIONS

Nrf2 activators are applicable for treating ocular diseases and novel Nrf2 activators have potential as a unique method for prevention and treatment of retinovascular disease.

Abbreviations

AU, arbitrary unit; BEACON study, bardoxolone methyl evaluation in patients with chronic kidney disease and type 2 diabetes: the occurrence of renal events; BEAM study, bardoxolone methyl treatment: renal function in chronic kidney disease/type 2 diabetes; CD, concentration to double NQO1 activity; CDDO, 2-cyano-3,12-dioxooleana-1,9(11)-dien-28-oic acid; Ct, threshold cycle; Keap1, Kelch-like ECH-associated protein 1; NQO1, NADPH:quinone oxidoreductase-1; Nrf2, nuclear factor erythroid 2-related factor 2; P, post-natal day; PLA, poly lactic acid; tBHP, *tert*-butyl hydroperoxide

Tables of Links

TARGETS
Enzymes
Cytochrome P450
Hmox1
Other protein targets
Kelch-like ECH-associated protein 1 (Keap1)

LIGANDS	
Bardoxolone methyl	Oleanolic acid
Dimethyl fumarate	Pravastatin
Hydrogen peroxide (H_2O_2)	RTA 408
LPS	Triamcinolone acetonide
	VEGF

These Tables list key protein targets and ligands in this article which are hyperlinked to corresponding entries in http://www.guidetopharmacology.org, the common portal for data from the IUPHAR/BPS Guide to PHARMACOLOGY (Pawson *et al.*, 2014) and are permanently archived in the Concise Guide to PHARMACOLOGY 2013/14 (Alexander *et al.*, 2013).

Introduction

Nuclear factor erythroid 2-related factor 2 (Nrf2) is expressed in many tissues, particularly those associated with detoxification (the liver and kidney) and those that are exposed to the external environment (skin, lungs and the gastrointestinal tract) (Itoh *et al.*, 2010; Suzuki *et al.*, 2013). Under basal resting conditions, Nrf2 is tethered within the cytosol by an adaptor protein, Kelch-like ECH-associated protein 1 (Keap1). Several cysteine residues in Keap1 serve as primary sensors for stress signals, and their modification leads to conformational changes in Keap1, thereby inducing the liberation of Nrf2. Activation of the Keap1-Nrf2 signalling pathway is expected to protect cells from a variety of stimuli such as reactive toxicants and pro-inflammatory factors. Several triterpenoids react with cysteine residues of Keap1 as Michael acceptors and thereby activate Keap1-Nrf2 signalling (Liby *et al.*, 2007; Liby and Sporn, 2012). It is in this context that a number of triterpenoids have been chemically synthesized and intensively tested for a long period (Sporn *et al.*, 2011). The most well-known triterpenoid is bardoxolone methyl [2-cyano-3,12-dioxooleana-1,9(11)-dien-28-oic acid (CDDO) methyl ester/CDDO-Me/RTA 402]. Oleanolic acid is commonly used as the starting material for synthetic oleanane triterpenoids and modifications at C17 position are often used to synthesize CDDO scaffolds such as imidazole (CDDO-Im), methyl amide (CDDO-MA), ethyl amide (CDDO-EA), trifluoroethyl amide (CDDO-TFEA) and nitrile (di-CDDO). These compounds have been reported to inhibit inflammatory mediators, induce cell differentiation and induce apoptosis of cancer cells *in vitro* and also to be effective in many pathological models (Liby and Sporn, 2012). In addition, one of the CDDO scaffolds, RTA 408, is currently being tested in clinical trials for the treatment of, for example, radiation-induced dermatitis (ClinicalTrials.gov identifier: NCT02142959) (Reisman *et al.*, 2014).

Bardoxolone methyl is called an oral antioxidant inflammation modulator, and the clinical data of Phase 2b were partially published in 2011 (Pergola *et al.*, 2011). The BEAM study (bardoxolone methyl treatment: renal function in chronic kidney disease/type 2 diabetes) evaluated the safety and efficacy of this compound in patients with moderate to severe chronic kidney disease associated with type 2 diabetes (227 patients, 52 weeks). Patients receiving bardoxolone methyl showed an increase in the estimated GFR at 24 weeks and the improvement persisted at 52 weeks. However, a higher cardiovascular mortality in the treatment arm (20 mg) in Phase 3 caused the BEACON study (bardoxolone methyl evaluation in patients with chronic kidney disease and type 2 diabetes: the occurrence of renal events) (1600 patients with stage 4 chronic kidney disease) to be terminated in 2012 (de Zeeuw *et al.*, 2013). Acute sodium and volume retention might be the cause of these adverse cardiovascular events (Chin *et al.*, 2014), but whether both the efficacy and adverse events associated with bardoxolone methyl are the result of Nrf2 activation is still debatable (Abboud, 2013). After the appearance of bardoxolone methyl, many chemically modified derivatives have been reported. Moreover, the activity of bardoxolone methyl is much more potent than that of sulforaphane, which was previously used as a benchmark for a Nrf2 activator (Kensler *et al.*, 2013). One solution for obtaining novel more promising Nrf2 activators is to change the method used from chemical modification to microbial transformation. The crude products obtained using the latter method normally contain many compounds; however, it is possible to obtain novel compounds that would be challenging to synthesize chemically (Venisetty and Ciddi, 2003; Ravindran *et al.*, 2012). The microorganisms used include fungus, actinomyces and bacterium.

Oxidative stress is considered to be one of the main initial determinants of cellular damage. Triterpenoids seem to be an attractive way to drive a broad range of antioxidant enzymes and combat deleterious phenomena, especially those related to age. Target organs include the brain, kidney, lung, eye, liver and heart (Liby and Sporn, 2012). Among them, ocular diseases are a promising target for triterpenoids because focal administration, such as intravitreal injection or eye drops, would lower the risks associated with systemically administered bardoxolone methyl.

In the present study novel Nrf2 activators were found from microbial transformation products using bardoxolone methyl as a parent compound. NADPH:quinone oxidoreductase-1 (NQO1) induction activity was first checked for screening the products. Cellular toxicity was investigated by measuring the release of LDH and mitochondrial dehydrogenase activity and related to an analysis of the chemical structures. The effects of the Nrf2 activators were also investigated in a model of oxygen-induced retinopathy, which is a well-accepted animal

model with features of retinopathy of prematurity (Akula *et al.*, 2007). Finally, we examined the effects of the compounds on blood–retinal barrier permeability in rabbits.

Methods

Animals and reagents

Pregnant Sprague-Dawley rats and New Zealand White rabbits were purchased from Charles River Laboratories (Kanagawa, Japan) and Oriental Yeast (Tokyo, Japan) respectively (totally 20 rats and 30 rabbits). All experimental procedures were performed in accordance with the in-house guideline of the Institutional Animal Care and Use Committee of Daiichi Sankyo. All animals received standard laboratory diet and filtered water *ad libitum* under specific pathogen-free conditions. Lights were switched on and off every 12 h and the room was maintained at 23°C. Every effort was made to minimize animal suffering and to reduce the number of animals employed. All animal studies were also conducted in accordance with the ARRIVE guidelines (Kilkenny *et al.*, 2010; McGrath *et al.*, 2010). Hepa1c1c7 cells (Cat. No. CRL-2026, a mouse hepatic epithelial cell line), ARPE-19 cells (Cat. No. CRL-2302, a human retinal pigment epithelial cell line) and RAW 264.7 cells (Cat. No. TIB-71, murine macrophage cell line) were purchased from ATCC (Manassas, VA, USA). RS compounds were prepared by biotransformation of bardoxolone methyl using the fungus *Chaetomium globosum* SANK 10312 isolated in our laboratory (Komoriya *et al.*, 2013). Briefly, this strain was grown in shake culture for 2 days in the FFA-1 medium (3% glycerin, 3% glucose, 2% soluble starch, 1% soybean meals, 0.25% gelatin, 0.25% yeast extract, 0.25% NH_4NO_3 and 0.01% anti-foaming agent) at 23°C, 210 r.p.m. on a shaker. Bardoxolone methyl dissolved in DMSO was added at a final concentration of 100 $\mu g \cdot mL^{-1}$, and the incubation was continued for 6 days. The whole broth was mixed with equivalent volume of acetone and then filtered. The filtrate was extracted with ethyl acetate (pH not adjusted) and washed with saturated NaCl solution. The upper layer was concentrated *in vacuo*. Finally, the crude extract was purified by HPLC preparation systems to obtain RS compounds. Poly lactic acid (PLA-0020, MW: 20 000) was purchased from Wako Pure Chemical Industries (Osaka, Japan). A sustained-release formulation (microspheres) of RS9 was prepared and characterized by a standard method (Wang and Burgess, 2012). Briefly, a solution of PLA and RS9 in dichloromethane was poured into aqueous solution containing PLA. With continuous stirring of the mixture, dichloromethane was evaporated to form PLA solid microspheres containing RS9. The mean diameter of the microsphere ranged from approximately 15–30 μm. Sustained release of RS9 from the microspheres was confirmed by an *in vitro* release test (data not shown). The following were also purchased: DL-sulforaphane, LPS, triamcinolone acetonide and glycated albumin from Sigma-Aldrich (St. Louis, MO, USA); dimethyl fumarate and *tert*-butyl hydroperoxide (tBHP) from Tokyo Chemical Industry (Tokyo, Japan); LDH-Cytotoxic Test from Wako Pure Chemical Industries; Cell Counting Kit-8 (WST-8 solution) from Dojindo Molecular Technologies (Kumamoto, Japan); Hydrogen Peroxide Cell-Based Assay Kit from Cayman Chemical (Ann Arbor, MI, USA); TransAM® Nrf2 from Active Motif, Inc. (Carlsbad, CA, USA); and Fluorescite® i.v. injection from Alcon (Personalvermittlung, Switzerland).

An NQO1 induction assay in Hepa1c1c cells

NQO1 activity was measured according to the method previously reported (Fahey *et al.*, 2004). Hepa1c1c cells were plated in 96-well plates at 10 000 cells per well and cultured in 100 μL of DMEM containing 10% FBS for 24 h. The medium was changed to a compound-containing medium and then maintained for a further 48 h. The following was prepared just before use: a lysis solution (0.8% digitonin and 2 mM EDTA), an assay solution (25 mM Tris–HCl, 0.01% Tween-20, 0.07% albumin, 2 $U \cdot mL^{-1}$ glucose-6-phosphate dehydrogenase, 5 μM FAD, 1 μM glucose 6-phosphate, 30 μM NADP, 0.03% MTT and 50 μM menadione) and a stop solution [0.3 mM dicoumarol and 5 mM K_2HPO_4 (pH 7.4)]. The medium was removed and 50 μL of lysis solution was added to each well. The cells were incubated for 10 min at 37°C. The plates were then placed on a shaker and agitated for 10 min at room temperature. Next, 200 μL of assay solution was added to each well, and the plates were incubated at room temperature for 5 min. The reaction was stopped by adding 50 μL per well of the stop solution. The absorbance at 490 nm was read by a plate reader. The values in the wells containing no compounds were normalized to 1 and the normalized data were plotted using GraphPad Prism 5 (GraphPad Software Inc., La Jolla, CA, USA) $\{Y = \text{bottom} + (\text{top} - \text{bottom}) \cdot [1 + 10^{(\log EC50 - X)}]^{-1}\}$. Concentrations of compounds that doubled NQO1 activity were calculated as CD values (nM).

LDH and WST-8 assays in ARPE-19 cells

ARPE-19 cells were plated in 96-well plates at 5000 cells per well in 50 μL of DMEM:F12 containing 10% FBS and cultured for 6 h. The medium containing compounds was added in a volume of 50 μL and then cells were maintained for another 16 h. The amount of LDH released was measured according to the manufacturer's manual. Similar experiments were also conducted in Hepa1c1c7 cells. For the WST-8 assay, ARPE-19 cells were plated in 96-well plates at 10 000 cells per well and cultured for 6 h. The medium was changed to compound-containing medium and then the cells were maintained for 16 h. Cellular viability was evaluated at this point to check compound-induced damage according to the manufacturer's manual. When testing tBHP-induced cellular damage, cells were cultured in a medium containing 300 μM tBHP and compounds for a further 6 h.

Evaluation of LPS-induced hydrogen peroxide in RAW 264.7 cells

RAW 264.7 cells were plated in 96-well plates at 80 000 cells per well in 100 μL of DMEM containing 10% FBS and cultured for 4 h. The cells were maintained in the compound-containing FBS-free medium for 4 h and then incubated with the compounds and 10 $ng \cdot mL^{-1}$ LPS-containing FBS-free medium for 2 days. Measurement of hydrogen peroxide in the medium and a WST-8 assay were conducted according to the manufacture's manual. To measure the translocation of Nrf2 protein to the nucleus, the cells were plated at 8.8×10^6 cells in 100 mm dishes. Preparation of the nucleus fraction was carried out following the kit's instructions.

Measurement of Nrf2-targeted genes in ARPE-19 cells and the retina

ARPE-19 cells were plated in 24-well plates at 60 000 cells per well with 500 μL of medium and cultured for 24 h. The medium was changed to compound-containing medium and cells were incubated for 6 h. The cells were used for collecting mRNA to synthesize cDNA. A quantitative PCR was performed using the real-time PCR HT7900 (Thermo Fisher Scientific, Waltham, MA, USA). The threshold cycle (Ct) of each transcript was normalized to the average Ct for housekeeping genes. Fold differences were determined by the $2^{-\Delta\Delta Ct}$ method.

Oxygen-induced retinopathy in rats

Sprague-Dawley neonatal pups were used for this experiment (Akula *et al.*, 2007). For each experiment, 14–16 pups were kept with a mother rat in each cage. Both male and female pups were used, and the compound-treated pups were randomly assigned based on weight on post-natal day 11 (P11). The weight on P11 was 14–19 g. Mother rats were rotated between the hyperoxia and room air conditions every 3 days during the experimental period for recovery from hyperoxia-induced stress. The pups were exposed from birth to P12 to daily cycles of 80% oxygen (21 h) and room air (3 h), and then maintained in room air from P12 to P18. RS9 was suspended in 0.5% methyl cellulose and the pups were dosed, p.o., once a day with the suspension at 10 mL·kg^{-1} from P11 to P17. In the case of intravitreous injection, RS9 microspheres in saline were injected in 2 μL on P11 using 33 gauge needles. Antibiotic drops were used after the injection. The pups were killed on P18 by carbon dioxide, and both eyes were enucleated and placed in 10% neutral buffered formalin overnight. From some pups, the retina was collected to obtain mRNA for a quantitative PCR. The fixed eye was washed with PBS and then the flat-mounted retina was used for ADPase staining (Zhang *et al.*, 2000). Staining buffer containing 0.1% $Pb(NO_3)_2$, 0.12% $MgCl_2$ and 0.1% ADP was prepared in 200 mM Tris maleate (pH 7.2) before use. The dissected retina was incubated in the staining buffer at 37°C for 30 min. Each retinal quadrant was divided by visual estimation into three equal parts (clock hours), and each clock hour was scored by masked examiners (blinded by N.Y. and then scored by T.I.) for the presence or absence of abnormal neovascularization (1 or 0) (Zhang *et al.*, 2000).

Blood–retinal barrier permeability in rabbits

In this experiment, male 4- to 6-month-old rabbits (n = 3–4 in each group, 3–4 kg) were used. Rabbits were randomly assigned to each group, and the compounds suspended in saline with or without 0.1 mg glycated albumin were intravitreously injected under anaesthesia (ketamin 25 mg·kg^{-1} and medetomidine 0.1 mg·kg^{-1}, intramuscular injection) at 50 μL by using 30 gauge needles from the sclera. Antibiotic drops were used after the injection (day 0). Two days after the intravitreous injection, fluorescein, 150 mg·1.5 mL^{-1} per animal, was injected i.v. One hour after the i.v. injection, rabbits were killed by pentobarbital, and the vitreous humor was collected for measuring fluorescence (day 2). The fluorescence reflects the sum of the blood–retinal barrier and blood–aqueous barrier. Rabbits were also used to measure the concentration of RS9 in the vitreous humor; they were intravitreously injected with RS9 (3 mM, 50 μL) and 0.1 mg of glycated albumin (n = 4 at each time point).

Statistical analysis

Summary statistics were calculated using Microsoft Excel 2010 (Microsoft, Redmond, WA, USA) and all graphs were created using GraphPad Prism 5. Data are shown as means ± SEM, and significance tests were conducted by the SAS System Release 9.2 (SAS Institute, Cary, NC, USA). Statistical analyses among multiple groups were performed by using one-way ANOVA, followed by the Dunnett's test or Tukey's test. For oxygen-induced retinopathy, the Steel test was conducted. $P < 0.05$ was considered significant.

Results

Novel Nrf2 activators are potent inducers of NQO1 activity in Hepa1c1c7 cells

RS compounds were purified from fermentation products in our laboratory. A typical HPLC chart and chemical structures employed in this study are shown in Figure 1A and B. A significant amount of sulforaphane is contained in the sprouts of broccoli. The cysteine residue of sulforaphane works as a weak electrophile and it interacts with cysteine residues of Keap1 as Michael acceptors. Dimethyl fumarate is also a weak electrophile and is approved for relapsing forms of multiple sclerosis (Gao *et al.*, 2014). Microbial biotransformation of bardoxolone methyl resulted in the production of novel Nrf2 activators (RS8, RS9, RS10, RS11, RS12 and RS14). The differences between bardoxolone methyl and the RS compounds were epoxidation at the A-ring and hydroxylation/ketonization at the E-ring. Nrf2 activity was evaluated by NQO1 induction activity in Hepa1c1c7 cells. RS compounds were slightly more potent or had comparable activity to bardoxolone methyl (Figure 2A and B). Among them, RS9 was the most potent and the concentration needed to double (CD) the specific Nrf-2 activity was 0.2 nM (CD values in Figure 1B). The CD values for bardoxolone methyl, sulforaphane and dimethyl fumarate were 0.9 nM, 154.4 nM and 13.3 μM respectively (Figure 2C). The cytotoxicity data are shown in Figure 2D–E.

RS9 inhibits tBHP-induced cellular damage in ARPE-19 cells

The effects bardoxolone methyl and RS9 on typical Nrf2-targeted genes were tested in ARPE-19 cells. Increased levels of the three tested genes were detected at lower concentrations of RS9 than bardoxolone methyl (Figure 3A–C). The change was most apparent in *Hmox1*, which is an enzyme known to have strong antioxidant effects. The addition of tBHP, a free radical generator, decreased cellular viability by approximately 40%, reflecting damage to mitochondrial functional activity (Figure 3D). Simultaneous treatment with bardoxolone methyl did not completely suppress this decrease in viability; however, RS9 inhibited the tBHP-induced cellular damage at 0.03 nM, and the viability was almost 100% at 0.3 nM. This effect was not observed in the triamcinolone acetonide-treated wells. The cytotoxicity of the Nrf2 activators was tested in an LDH assay of ARPE-19 cells. Among the RS compounds, RS8 and RS9 showed substantially less cytotoxicity compared with bardoxolone

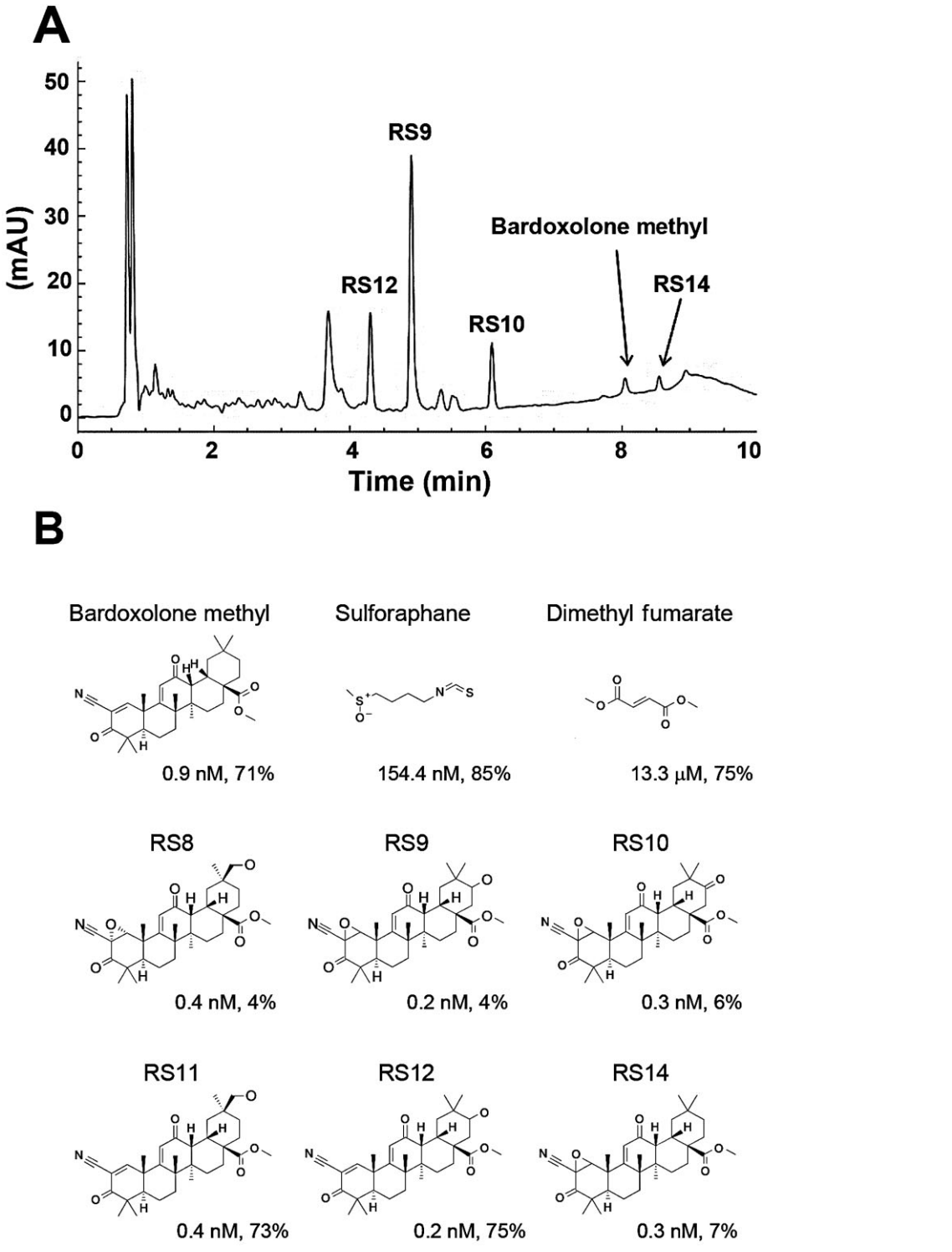

Figure 1

Chemical structures of Nrf2 activators. (A) The HPLC chart of ethyl acetate extract. Imtakt Unison UK-C18 (4.6 × 75 mm, 3 μm), (A) 10 mM ammonium formate (containing 0.01% formic acid), (B) acetonitrile (containing 0.01% formic acid), B (%): 50–90 per 7 min, 90 per 7–9 min, flow rate: 1.0 mL·min^{-1}, 10 μL injection, detection: UV 230 nm. mAU, milli-arbitrary unit. (B) Chemical structures. CD values (Hepa1c1c7 cells, 48 h, see Figure 2A–C) and cytotoxicity at 200 μM (ARPE-19 cells, 16 h, see Figure 3E–F) are shown for all compounds.

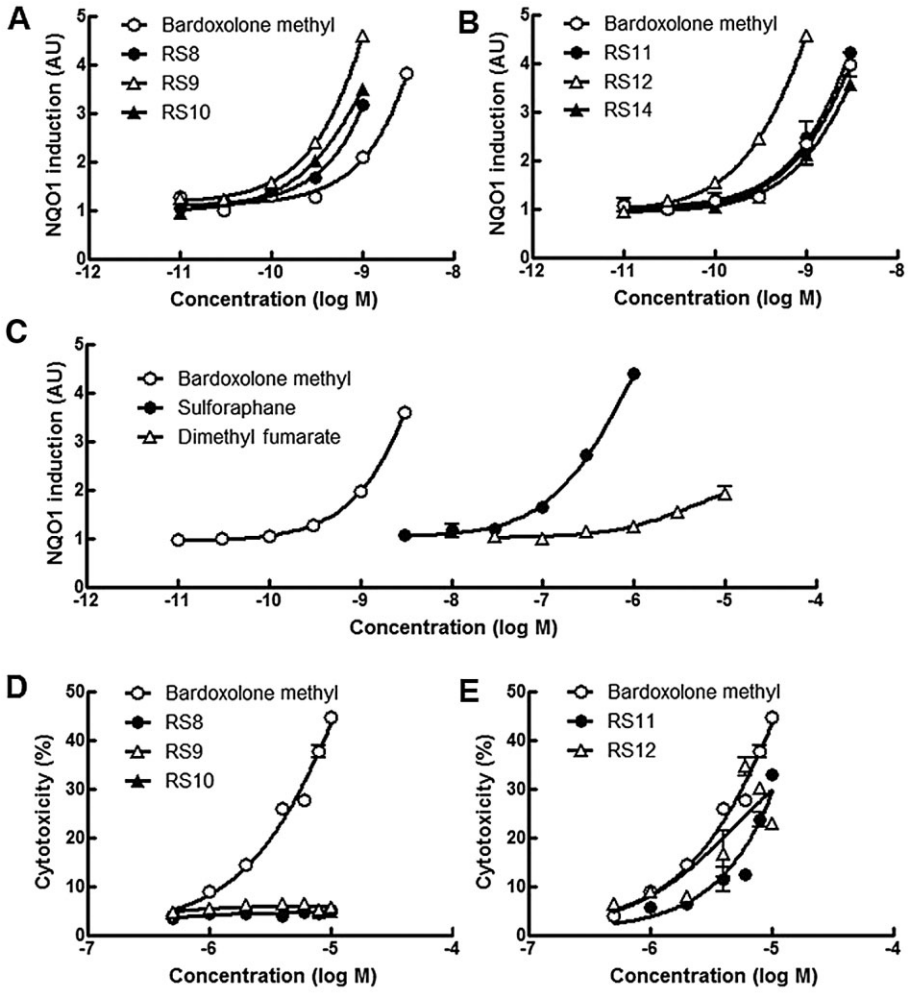

Figure 2

NQO1 activity induced by Nrf2 activators and an LDH assay in Hepa1c1c7 cells. (A–C) Hepa1c1c7 cells were treated with the compounds for 48 h and CD values are shown in Figure 1B. Experiments were conducted in triplicate. Bardoxolone methyl was set in all plates as a reference. $P < 0.05$ versus bardoxolone methyl: RS8 (30 pM), RS9 (100 pM), RS10 (30 pM), RS12 (30 pM); $P < 0.01$ versus bardoxolone methyl: RS8 (300 pM, 1 nM), RS9 (30 pM, 300 pM, 1 nM), RS10 (300 pM, 1 nM) and RS12 (100 pM, 300 pM), Dunnett's test. (D–E) Hepa1c1c7 cells were treated with compounds for 16 h. Experiments were conducted in triplicate. $P < 0.05$ versus bardoxolone methyl: RS8 (8 μM, 10 μM), RS9 (10 μM), RS10 (2 μM, 4 μM, 8 μM, 10 μM), RS11 (1 μM, 4 μM), RS12 (0.5 μM); $P < 0.01$ versus bardoxolone methyl: RS8 (1 μM, 2 μM, 4 μM, 6 μM), RS11 (2 μM, 8 μM), RS12 (10 μM), Dunnett's test.

Figure 3

Effects of Nrf2 activators on Nrf2-targeted genes and cytotoxicity in ARPE-19 cells. (A–C) Changes in Nrf2-targeted genes in ARPE-19 cells. Bardoxolone methyl and only RS9 were tested in this study, and ARPE-19 cells were treated with the compounds for 6 h. (D) Effects on tBHP-induced cellular damage in ARPE-19 cells. Addition of 300 μM tBHP for 6 h decreased cellular viability by 40% (from an open circle to a closed circle). Only RS9 completely inhibited tBHP-induced cellular damage (closed triangles). Experiments were conducted in triplicate. $^{**}P < 0.01$ versus no tBHP, $^{\dagger\dagger}P < 0.01$ versus tBHP, Tukey's test. (E–F) Cytotoxicity of RS compounds in ARPE-19 cells. ARPE-19 cells were treated with compounds for 16 h. Note that cytotoxicity was substantially decreased for RS8 and RS9. Experiments were conducted in triplicate and data from five plates are summarized. The averaged data for bardoxolone methyl in (A) were also plotted in (B) for comparison. $^{**}P < 0.01$ versus bardoxolone methyl: RS8 (all concentrations), RS9 (all concentrations), sulforaphane (except three high concentrations) and dimethyl fumarate (all concentrations), Dunnett's test. (G–H) Effects of RS compounds on cellular viability in ARPE-19 cells. ARPE-19 cells were treated with compounds for 16 h. Experiments were conducted in triplicate and data from four plates are summarized. The averaged data of bardoxolone methyl in (G) are also plotted in (H) for comparison. $P < 0.05$ versus bardoxolone methyl: dimethyl fumarate (the lowest concentration); $^{**}P < 0.01$ versus bardoxolone methyl: RS8 (all concentrations), RS9 (all concentrations), RS10 (all concentrations), sulforaphane (except the highest concentration) and dimethyl fumarate (except the lowest concentration), Dunnett's test.

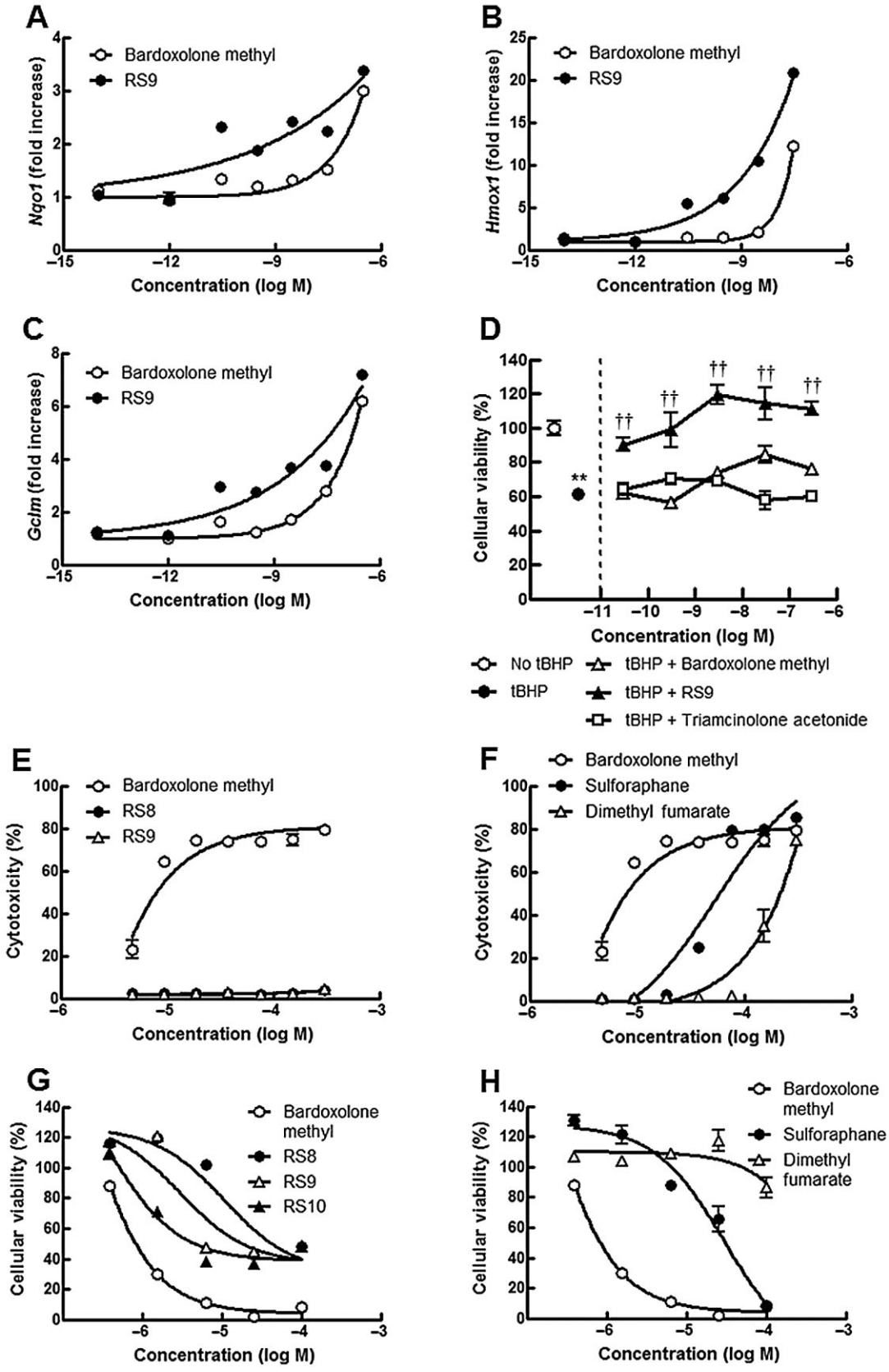
A
Bardoxolone methyl
RS9
Nqo1 (fold increase)
Concentration (log M)
B
Bardoxolone methyl
RS9
Hmox1 (fold increase)
Concentration (log M)
C
Bardoxolone methyl
RS9
Gclm (fold increase)
Concentration (log M)
D
Cellular viability (%)
Concentration (log M)
No tBHP
tBHP
tBHP + Bardoxolone methyl
tBHP + RS9
tBHP + Triamcinolone acetonide
E
Bardoxolone methyl
RS8
RS9
Cytotoxicity (%)
Concentration (log M)
F
Bardoxolone methyl
Sulforaphane
Dimethyl fumarate
Cytotoxicity (%)
Concentration (log M)
G
Bardoxolone methyl
RS8
RS9
RS10
Cellular viability (%)
Concentration (log M)
H
Bardoxolone methyl
Sulforaphane
Dimethyl fumarate
Cellular viability (%)
Concentration (log M)

methyl (Figure 3E). Large quantities of LDH were observed to be released in the presence of 300 μM sulforaphane (Figure 3F). The sensitivity of detecting cellular damage using WST-8 solution is generally higher than that of the LDH assays, although the output reflects many factors. Similar phenomena were observed between bardoxolone methyl and RS compounds in the LDH assays (Figure 3G). The viability was maintained only in dimethyl fumarate up to 100 μM (Figure 3H). Below 100 nM, all compounds showed almost no cytotoxicity, and similar dose-responses were also obtained in Hepa1c1c7 cells (data not shown).

RS9 inhibits LPS-induced hydrogen peroxide production in RAW 264.7 cells

To further investigate the protective effects of the Nrf-2 activators against oxidative stress and inflammation, we measured LPS-induced hydrogen peroxide production in RAW 264.7 cells. The addition of 10 ng·mL^{-1} LPS induced the production of hydrogen peroxide, bardoxolone methyl and RS9 significantly suppressed this increase at a concentration of 100 nM (Figure 4A). These results are consistent with previously reported findings that silencing Nrf2 exaggerates LPS-induced inflammatory responses in the human monocytic cell line THP-1 (Rushworth *et al.*, 2008). In the same experimental conditions, after 48 h of treatment, cellular viability was significantly reduced at concentrations of bardoxolone methyl greater than 10 nM (Figure 4B). Translocation of the Nrf2 protein to the nucleus without LPS was also investigated and the increase was significant in the presence of 100 nM of both compounds (Figure 4C). The protein level was higher in the bardoxolone methyl-treated cells and similar results were obtained in LPS-treated experiments (data not shown).

RS9 increases Nrf2-targeted genes in the retina

The mRNA changes in the retina of rat pups were examined after repeated oral administration of RS9. The tissues were collected in the oxygen-induced retinopathy experiments. The increases in *nqo1* and *hmox1* were significant in the retina; however, the level of *gclm* did not change (Figure 5A–C). Significant increases in *nqo1* and *gclm* were also detected when the liver was tested (data not shown).

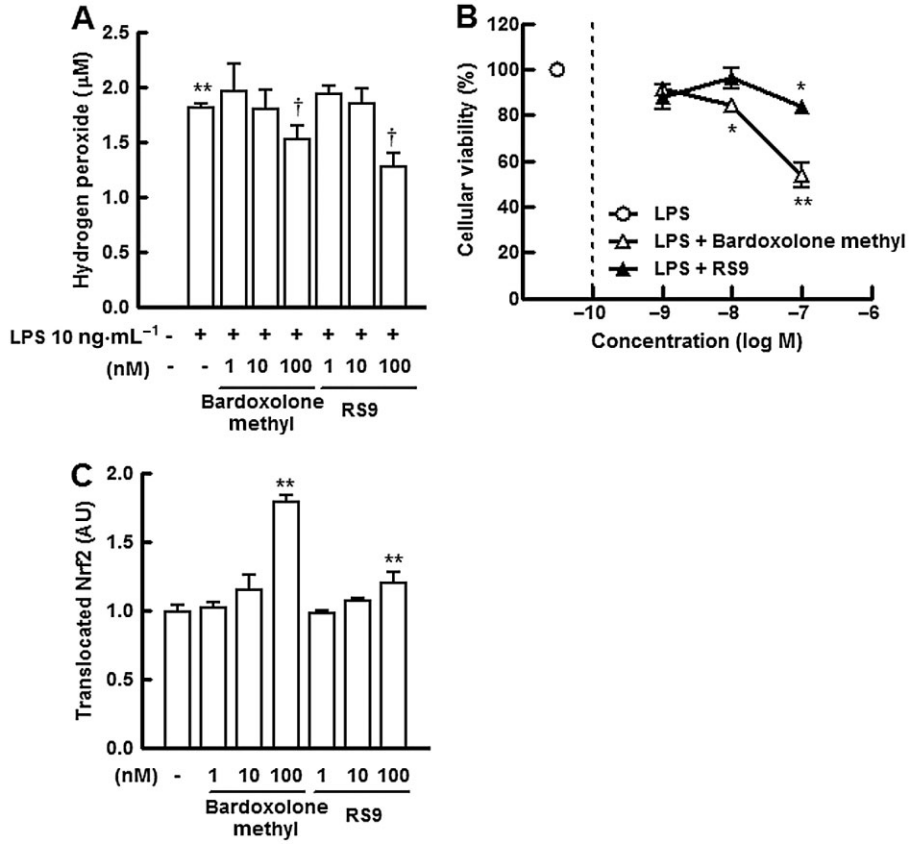

Figure 4

Effects of RS9 on cellular damage induced by LPS in RAW 264.7 cells. (A) Effects of bardoxolone methyl and RS9 on LPS-induced increase in hydrogen peroxide in RAW 264.7 cells. Addition of 10 ng·mL^{-1} LPS increased the production of hydrogen peroxide, and treatment with the compounds for 48 h suppressed the increase. Triplicate results, $^{**}P < 0.01$ versus no LPS, †$P < 0.05$ versus LPS without compounds, Tukey's test. (B) Effects of compounds on cellular viability in LPS-treated RAW 264.7 cells. Experimental conditions were the same as in Figure 3G. Triplicate results, $^{*}P < 0.05$, $^{**}P < 0.01$ versus LPS only, Dunnett's test. (C) Translocation of Nrf2 protein to the nucleus in RAW 264.7 cells. An increase in translocated Nrf2 was observed in both groups. $^{**}P < 0.01$ versus no compounds, Dunnett's test.

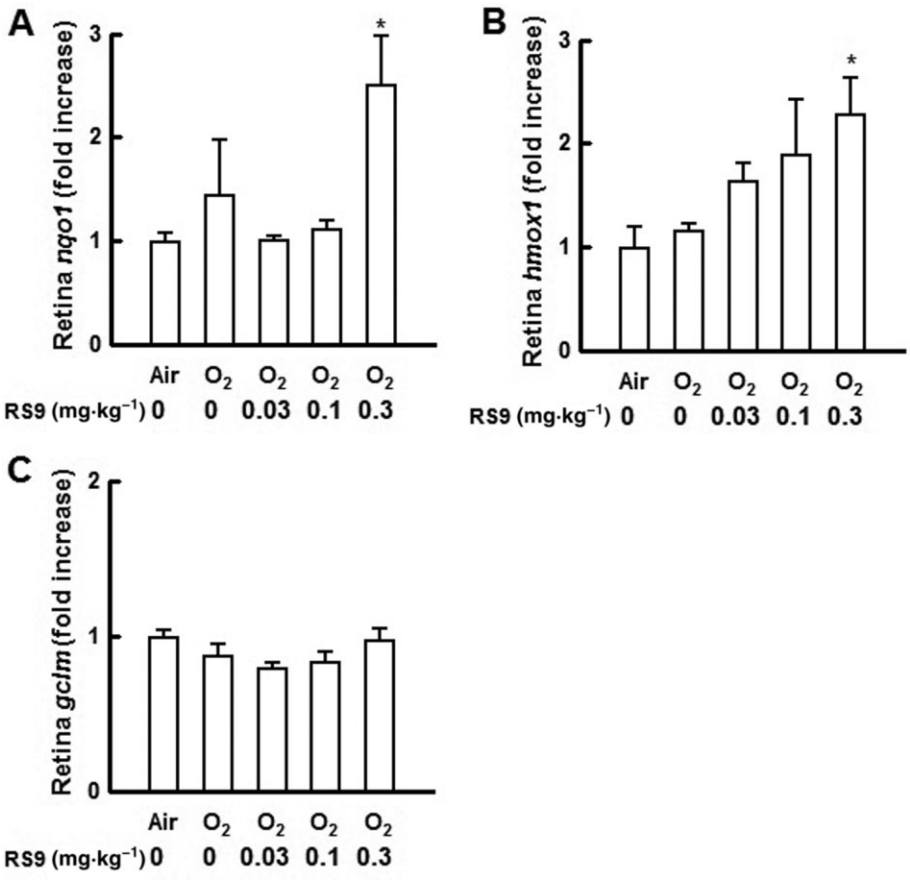

Figure 5

Effects of RS9 on Nrf2-targeted genes in the retina. (A–C) Changes in Nrf2-targeted genes in the retina after repeated oral administration of RS9. Rat pups were orally administered RS9 once a day from P11 to P17, and the retina was obtained on P18. *$P < 0.05$ versus air-exposed vehicle-administered rats, Dunnett's test, $n = 4$.

RS9 suppresses oxygen-induced retinopathy in rats

Repeated oral administration of RS9 induced a dose-dependent reduction in the extent (clock hours) of neovascularization compared with vehicle-administered groups (Figure 6A, $n = 7$ for 0.03 mg·kg^{-1}, 14 for 0.1 mg·kg^{-1} and 15 for the rest groups). The P value at a dose of 0.3 mg·kg^{-1} was 0.066 (vs. air-exposed vehicle-administered rats, Steel test). Toxic effects were not observed during the oral administration; these were assessed by body weight and health status check (data not shown). Sustained release formulations (microspheres) were prepared using PLA-0020 as a base, which consisted of RS9 and PLA-0020 with the ratio of 1:9 (w w^{-1}). Intravitreal administration of RS9 (2 nmol·1.6 μL^{-1} per eye) showed a tendency to inhibit the pathological scores (Figure 6B, $n = 8$ for all groups).

RS9 inhibits blood–retinal barrier permeability in rabbits

All the rabbits were in good health before the experiments, and treatment with the compounds did not induce any adverse events including ocular surface inflammation. Intravitreal injection of glycated albumin (0.1 mg·50 μL^{-1} per eye) increased blood–retinal barrier permeability 48 h after the injection, suggesting that it induced acute inflammation (Figure 6C, $n = 3$ for 0.3 mM and 4 for the rest groups). Simultaneous injection of RS9 significantly inhibited the permeability at a dose of 0.3 mM. Bardoxolone methyl was also tested in the same protocol; however, it did not show any inhibitory effects (Figure 6D, $n = 3$ for RS9 0.03 mM and bardoxolone methyl 0.1 mM, and 4 for the rest groups), and moreover it increased the permeability at a dose of 3 mM (data not shown), indicating that its safety margin is narrow. Finally, the pharmacokinetic data of RS9 (3 mM, 50 μL, lower limit of quantification: 3 pM) in the vitreous humor were also obtained. Although RS9 was prepared in the form of a microsphere the concentration was 49 nM 24 h after intravitreal injection (Figure 6E). These results imply that the concentration is around one-tenth of 49 nM in the case of 0.3 mM injection; moreover, the concentration in the retina seems below this.

Discussion and conclusions

A biotransformation technique was applied to obtain bardoxolone methyl derivatives and we succeeded in obtaining RS9,

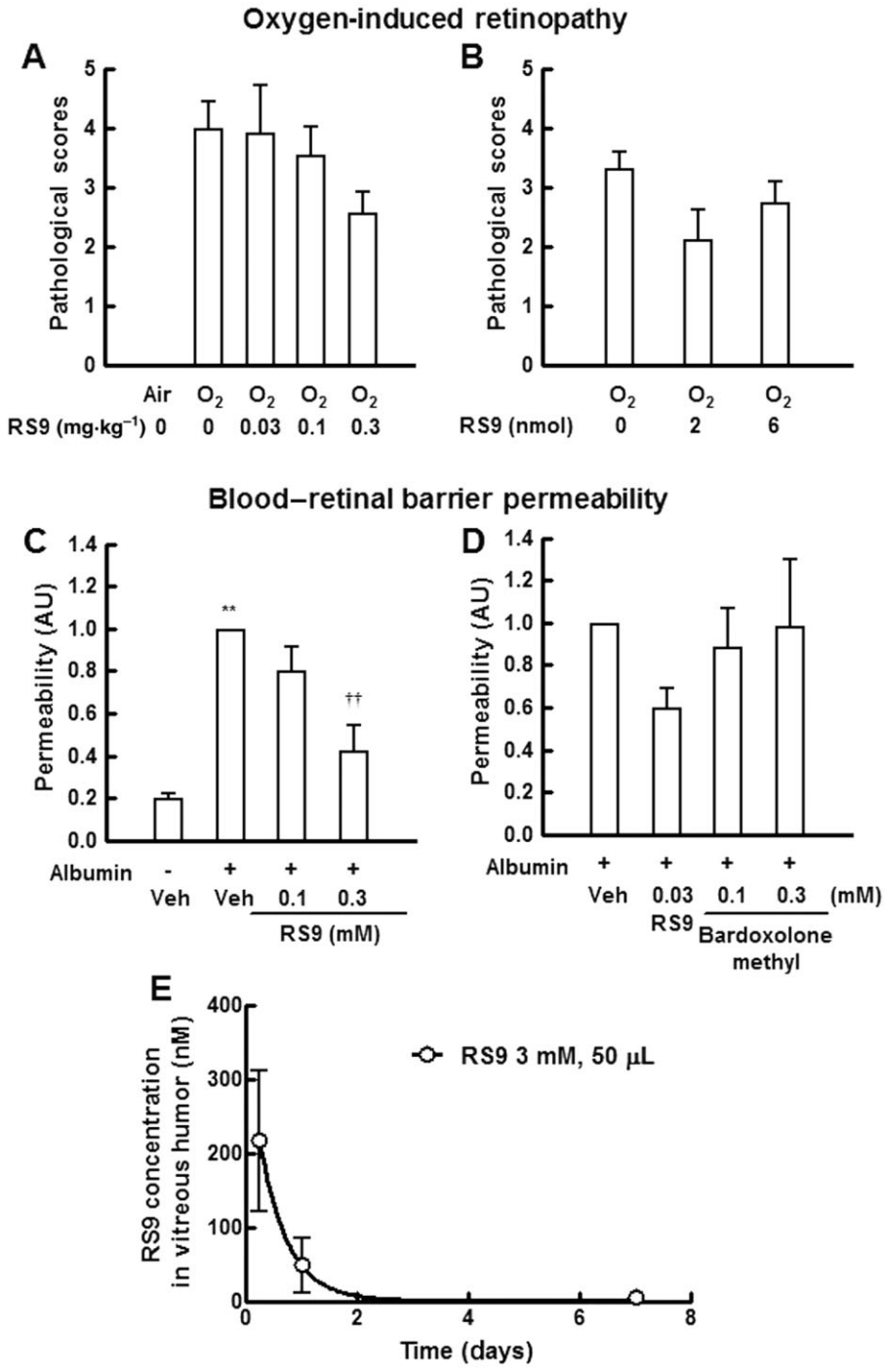

Figure 6

Effects of RS9 on oxygen-induced retinopathy in rats and blood–retinal barrier permeability in rabbits. (A) Effects of orally administered RS9 on pathological scores. Rat pups were orally dosed with RS9 once a day from P11 to P17, and the retina was obtained on P18. The *P* value at a dose of 0.3 mg·kg^{-1} was 0.066 (vs. air-exposed vehicle-administered rats, Steel test). (B) Effects of injected RS9 microspheres. Microspheres were injected once on P11. Each clock hour was scored for the presence or absence of abnormal neovascularization (1 or 0). Scores were evaluated blindly throughout the experiments, n = 7–15. (C, D) Inhibitory effects of intravitreally injected RS9 suspension on glycated albumin-induced leakage. RS9 and albumin were intravitreally injected on Day 0, and the fluorescence was measured on day 2. **P < 0.01 versus no albumin and vehicle-injected rabbits, ††P < 0.01 versus albumin and vehicle-injected rabbits, Tukey's test, P = 3–4. (E) Pharmacokinetic data for RS9 in the vitreous humor. RS9 (3 mM, 50 µL) was injected with glycated albumin, n = 4.

which has stronger NQO1 induction activity and less cytotoxicity compared with bardoxolone methyl. A comparison of the RS compounds suggests that epoxidation in the A-ring (RS9 and RS12) contributes to a reduction in cytotoxicity, and hydroxylation in the E-ring (RS9 and RS14) is involved in the improvement in activity. Bardoxolone methyl is chemically synthesized from oleanolic acid. The fermentation products of oleanolic acid with *Cunninghamella blakesleeana* were originally reported in 1969 (Hikino *et al.*, 1969; 1972). Interestingly, the hydroxylation sites are very different in the case of oleanolic acid and bardoxolone methyl when using *Cunninghamella* genera (the B- or C-rings in oleanolic acid, and the E-ring in bardoxolone methyl). This simple structure–activity/toxicity relationship should be studied further to optimize RS compounds.

Biotransformation is a chemical reaction that is catalysed by whole cells (microorganisms, plant cells, animal cells, etc.) or by isolated enzymes and would provide difficult-to-synthesize drugs (Venisetty and Ciddi, 2003; Ravindran *et al.*, 2012). This approach has several advantages that are superior to the traditional chemical synthesis. Firstly, if successful, some of the compounds obtained will have increased activity and decreased toxicity compared with parent compounds, as demonstrated in this report. It is helpful to analyse the metabolites from parent compounds, especially glutathione adducts, for conducting additional modifications at the specified sites to reduce toxicity. In addition to activity and toxicity, some products might be well-balanced in bioavailability and clearance. Secondly, when the best whole cells or isolated enzymes are selected, the production rate is normally higher and the by-products are usually fewer than those of a chemical reaction. Lastly, biological transformation is conducted in mild conditions, which might be an important factor from the point of view of reproducibility. We possess a variety of microorganism libraries for drug discovery to identify new biologically-active natural products. One successful example is the discovery of the world's first statins from *Penicillium citrinum*, obtained by examining over 6000 microorganisms in 1976 (Endo *et al.*, 1976). Statins competitively inhibit 3-hydroxy-3-methyl-glutaryl coenzyme A reductase to reduce cholesterol biosynthesis, and this finding resulted in the approval of pravastatin (Serizawa and Matsuoka, 1991). In addition, the microorganism biotransformation, hydroxylation of ML-236B (compactin), became an established method in the initial phase of the development of pravastatin because of the disadvantages encountered with other methods, high cost and stereoisomer by-products with the chemical synthesis. In this study, the current conversion ratio for RS9 is around 50% 6 days after incubation of bardoxolone methyl with several kinds of fungus. We have screened over 3000 strains of microorganisms and are continuing to optimize the culture conditions to obtain RS9 more efficiently (data not shown). Moreover, we are trying to identify enzymes involved in the reaction including cytochrome P450, and these procedures would be used for industrial scale production in the future.

Nrf2-targeted genes were increased by around 0.03 nM of RS9 and this increase is consistent with the result that its protective effects against tBHP-induced cellular damage were also observed at 0.03 nM in ARPE-19 cells. Which genes mainly correlated to the protective effects remains to be investigated further and whether the same phenomenon in primary retinal cells is in the same range is also to be confirmed. Because of the identical mechanisms of bardoxolone methyl and RS9, it is likely that both compounds are protective against tBHP-induced cellular damage; however, only RS9 was effective in the range of 0.03–300 nM. This result reflects the lower cytotoxicity of RS9 compared with bardoxolone methyl, which seems critically important when launching clinical trials. Triamcinolone acetonide is used to treat many ocular diseases including diabetic retinopathy, wet-type aged macular degeneration and uveitis by intravitreous injection (Kiernan and Mieler, 2012); however, tBHP-induced cellular damage was not inhibited by triamcinolone acetonide in ARPE-19 cells. This result implies that steroids are not an appropriate remedy under the circumstances when oxidative stress is a causative factor.

Although excessive generation of reactive oxygen species and the resulting inflammation are involved in the development and progression of many diseases, approaches using traditional antioxidants in clinical studies have largely failed mainly because of the very short half-life of antioxidants (Firuzi *et al.*, 2011). To overcome this issue, activation of the Nrf2 pathway by triterpenoids seems to be a promising strategy, as it drives the expression and activity of many endogenous antioxidant and cytoprotective genes (Gao *et al.*, 2014). Indeed, several triterpenoids including bardoxolone methyl are known to be effective in a wide variety of disease models (Liby and Sporn, 2012). We focused upon ocular diseases because retinal photoreceptors contain a high content of polyunsaturated fatty acids caused by the high level of oxygen in the eye and sunlight exposure (Jarrett and Boulton, 2012; Payne *et al.*, 2014). The accumulation of oxidative stress-damaged cells also results in apoptosis and inflammation. If apoptotic cells are not rapidly removed, these cells undergo secondary necrosis and trigger the innate immune system in the retina. In this study, we demonstrated that oral administration of RS9 inhibits neovascularization in oxygen-induced retinopathy of rats, and intravitreal injection of RS9 suppressed permeability in glycated albumin-injected rabbits. The significance of our findings should correlate to the following reports: (i) Nrf2 knockout mice showed early onset of a blood–retina barrier breakdown, and the dysfunction was exacerbated in diabetes conditions (Xu *et al.*, 2014) and cigarette smoke exposure (Wang *et al.*, 2014); (ii) decreased DNA-binding activity of Nrf2 was reported in the retina of patients with diabetic retinopathy (Zhong *et al.*, 2013); (iii) glycated albumin is associated with microvascular complications including diabetic retinopathy (Nathan *et al.*, 2014), and is also used to investigate biogenesis of drusen in an aged macular degeneration model of rabbits (Yasukawa *et al.*, 2007); (iv) anti-oxidant oral supplements were shown to delay the progress of dry-type aged macular degeneration (Age-Related Eye Disease Study 2 Research Group, 2013); (v) vitamin A supplementation works for infants at risk of retinopathy of prematurity (Mactier, 2012); and (vi) drugs targeting VEGF are the mainstay of therapy to retard retinal neovascularization such as wet-type aged macular degeneration and diabetic macular oedema (Nguyen *et al.*, 2013); however, new drugs beyond anti-VEGF antibodies are strongly required because the therapy is not sufficient to cure all symptoms. Because it is likely that oxidative stress, the

Nrf2 system and consequent inflammation play important roles in the progression of the above diseases, our *in vivo* data suggest that Nrf2 activators are effective against oxidative stress-related ocular diseases when enough compounds remain in the vitreous humor or the retina. With regard to our results obtained after intravitreal injection of the compounds in oxygen-induced retinopathy, our microspheres need to be completed to achieve the final goal; more elaborate microspheres or implants are needed for a successful and reasonable method for future formulations (Kuno and Fujii, 2010).

Although pharmacokinetic data for bardoxolone methyl in humans are not available, cardiovascular adverse events in clinical trials were reported (Pergola *et al.*, 2011; de Zeeuw *et al.*, 2013). In the experiment of Figure 6C, no RS9 was apparent in the blood flow after its intravitreal injection during the experiments (lower limit of quantification: 3 pM), suggesting that the level of RS9 leaked does not induce any systemic adverse events. In addition, the leaked level of anti-VEGF antibodies after intravitreal injection has the potential to cause systemic adverse events (Falavarjani and Nguyen, 2013). The concentrations of RS9 in the vitreous humor were also examined: 217 nM at 6 h and 49 nM at 24 h after an injection of 3mM RS9 (in 50 μL) (Figure 6E). This range was almost non-toxic (Figures 2D, 3E, 3G and 4B); however, compared with *in vitro* experiments (Figures 3D and 4A), it seems that higher concentrations are needed to show significant *in vivo* pharmacological effects. This point should be investigated further including permeability to the tissue, *in vivo* stability of compounds, etc.

In conclusion, we discovered the novel Nrf2 activator, RS9, using a biotransformation technique. Because hydroxylation at specific sites of the E-ring is almost impossible to achieve using a chemical reaction, the originality of the compounds obtained here seems extremely high. Although *in vivo* pharmacological and toxicological studies are certainly needed, our data could help provide novel compounds for the treatment of retinovascular diseases.

Author contributions

Y. N., E. H., T. I. and T. M. performed the research; K. M., M. I., Y. O., T. O., Y. M., M. I., K. Y., Y. K. and S. K. contributed essential reagents or tools; Y. N. designed the research study, analysed the data and wrote the paper.

Conflict of interest

None.

References

Abboud HE (2013). Synthetic oleanane triterpenoids: magic bullets or not? Kidney Int 83: 785–787.

Age-Related Eye Disease Study 2 Research Group (2013). Lutein + zeaxanthin and omega-3 fatty acids for age-related macular degeneration: the Age-Related Eye Disease Study 2 (AREDS2) randomized clinical trial. JAMA 309: 2005–2015.

Akula JD, Hansen RM, Martinez-Perez ME, Fulton AB (2007). Rod photoreceptor function predicts blood vessel abnormality in retinopathy of prematurity. Invest Ophthalmol Vis Sci 48: 4351–4359.

Alexander SPH, Benson HE, Faccenda E, Pawson AJ, Sharman JL, Spedding M *et al.* (2013). The Concise Guide to PHARMACOLOGY 2013/14: Enzymes. Br J Pharmacol 170: 1797–1867.

Chin MP, Reisman SA, Bakris GL, O'Grady M, Linde PG, McCullough PA *et al.* (2014). Mechanisms contributing to adverse cardiovascular events in patients with type 2 diabetes mellitus and stage 4 chronic kidney disease treated with bardoxolone methyl. Am J Nephrol 39: 499–508.

Endo A, Kuroda M, Tsujita Y (1976). ML-236A, ML-236B, and ML-236C, new inhibitors of cholesterogenesis produced by *Penicillium citrinum*. J Antibiot 29: 1346–1348.

Fahey JW, Dinkova-Kostova AT, Stephenson KK, Talalay P (2004). The 'Prochaska' microtiter plate bioassay for inducers of NQO1. Methods Enzymol 382: 243–258.

Falavarjani KG, Nguyen QD (2013). Adverse events and complications associated with intravitreal injection of anti-VEGF agents: a review of literature. Eye (Lond) 27: 787–794.

Firuzi O, Miri R, Tavakkoli M, Saso L (2011). Antioxidant therapy: current status and future prospects. Curr Med Chem 18: 3871–3888.

Gao B, Doan A, Hybertson BM (2014). The clinical potential of influencing Nrf2 signaling in degenerative and immunological disorders. Clin Pharmacol 6: 19–34.

Hikino H, Nabetani S, Takemoto T (1969). [Microbial transformation of oleanolic acid. 1]. Yakugaku Zasshi 89: 809–813.

Hikino H, Nabetani S, Takemoto T (1972). [Microbial transformation of oleanolic acid. 4]. Yakugaku Zasshi 92: 1528–1533.

Itoh K, Mimura J, Yamamoto M (2010). Discovery of the negative regulator of Nrf2, Keap1: a historical overview. Antioxid Redox Signal 13: 1665–1678.

Jarrett SG, Boulton ME (2012). Consequences of oxidative stress in age-related macular degeneration. Mol Aspects Med 33: 399–417.

Kensler TW, Egner PA, Agyeman AS, Visvanathan K, Groopman JD, Chen JG *et al.* (2013). Keap1-nrf2 signaling: a target for cancer prevention by sulforaphane. Top Curr Chem 329: 163–177.

Kiernan DF, Mieler WF (2012). Intraocular corticosteroids for posterior segment disease: 2012 update. Expert Opin Pharmacother 13: 1679–1694.

Kilkenny C, Browne W, Cuthill IC, Emerson M, Altman DG (2010). Animal research: reporting *in vivo* experiments: the ARRIVE guidelines. Br J Pharmacol 160: 1577–1579.

Komoriya S, Nakagami Y, Hatano E, Ohnuki T, Masuda K, Iizuka M *et al.* (2013). Tripernoid derivatives. WO2014/148455 A1.

Kuno N, Fujii S (2010). Biodegradable intraocular therapies for retinal disorders: progress to date. Drugs Aging 27: 117–134.

Liby KT, Sporn MB (2012). Synthetic oleanane triterpenoids: multifunctional drugs with a broad range of applications for prevention and treatment of chronic disease. Pharmacol Rev 64: 972–1003.

Liby KT, Yore MM, Sporn MB (2007). Triterpenoids and rexinoids as multifunctional agents for the prevention and treatment of cancer. Nat Rev Cancer 7: 357–369.

Mactier H, McCulloch DL, Hamilton R, Galloway P, Bradnam MS, Young D *et al*. (2012). Vitamin A supplementation improves retinal function in infants at risk of retinopathy of prematurity. J Pediatr 160: 954–959.

McGrath J, Drummond G, McLachlan E, Kilkenny C, Wainwright C (2010). Guidelines for reporting experiments involving animals: the ARRIVE guidelines. Br J Pharmacol 160: 1573–1576.

Nathan DM, McGee P, Steffes MW, Lachin JM, DCCT/EDIC Research Group (2014). Relationship of glycated albumin to blood glucose and HbA1c values and to retinopathy, nephropathy, and cardiovascular outcomes in the DCCT/EDIC study. Diabetes 63: 282–290.

Nguyen DH, Luo J, Zhang K, Zhang M (2013). Current therapeutic approaches in neovascular age-related macular degeneration. Discov Med 15: 343–348.

Pawson AJ, Sharman JL, Benson HE, Faccenda E, Alexander SP, Buneman OP *et al*.; NC-IUPHAR (2014). The IUPHAR/BPS Guide to PHARMACOLOGY: an expert-driven knowledgebase of drug targets and their ligands. Nucl Acids Res 42 (Database Issue): D1098–D1106.

Payne AJ, Kaja S, Naumchuk Y, Kunjukunju N, Koulen P (2014). Antioxidant drug therapy approaches for neuroprotection in chronic diseases of the retina. Int J Mol Sci 15: 1865–1886.

Pergola PE, Raskin P, Toto RD, Meyer CJ, Huff JW, Grossman EB *et al*. (2011). Bardoxolone methyl and kidney function in CKD with type 2 diabetes. N Engl J Med 365: 327–336.

Ravindran S, Basu S, Surve P, Lonsane G, Sloka N (2012). Significance of biotransformation in drug discovery and development. J Biotechnol Biomater S13: 005.

Reisman SA, Lee CY, Meyer CL, Proksch JW, Sonis ST, Ward KW (2014). Topical application of the synthetic triterpenoid RTA 408 protects mice from radiation-induced dermatitis. Radiat Res 181: 512–520.

Rushworth SA, MacEwan DJ, O'Connell MA (2008). Lipopolysaccharide-induced expression of NAD(P)H:quinone oxidoreductase 1 and heme oxygenase-1 protects against excessive inflammatory responses in human monocytes. J Immunol 181: 6730–6737.

Serizawa N, Matsuoka T (1991). A two component-type cytochrome P-450 monooxygenase system in a prokaryote that catalyzes hydroxylation of ML-236B to pravastatin, a tissue-selective inhibitor of 3-hydroxy-3-methylglutaryl coenzyme A reductase. Biochim Biophys Acta 1084: 35–40.

Sporn MB, Liby KT, Yore MM, Fu L, Lopchuk JM, Gribble GW (2011). New synthetic triterpenoids: potent agents for prevention and treatment of tissue injury caused by inflammatory and oxidative stress. J Nat Prod 74: 537–545.

Suzuki T, Motohashi H, Yamamoto M (2013). Toward clinical application of the Keap1-Nrf2 pathway. Trends Pharmacol Sci 34: 340–346.

Venisetty RK, Ciddi V (2003). Application of microbial biotransformation for the new drug discovery using natural drugs as substrates. Curr Pharm Biotechnol 4: 153–167.

Wang L, Kondo N, Cano M, Ebrahimi K, Yoshida T, Barnett BP *et al*. (2014). Nrf2 signaling modulates cigarette smoke-induced complement activation in retinal pigmented epithelial cells. Free Radic Biol Med 70: 155–166.

Wang Y, Burgess D (2012). Long acting injections and implants. In: Wright JC, Burgess D (eds). Advances in Delivery Science and Technology. Springer: Heidelberg, pp. 167–194.

Xu Z, Wei Y, Gong J, Cho H, Park JK, Sung ER *et al*. (2014). NRF2 plays a protective role in diabetic retinopathy in mice. Diabetologia 57: 204–213.

Yasukawa T, Wiedemann P, Hoffmann S, Kacza J, Eichler W, Wang YS *et al*. (2007). Glycoxidized particles mimic lipofuscin accumulation in aging eyes: a new age-related macular degeneration model in rabbits. Graefes Arch Clin Exp Ophthalmol 245: 1475–1485.

de Zeeuw D, Akizawa T, Audhya P, Bakris GL, Chin M, Christ-Schmidt H *et al*. (2013). Bardoxolone methyl in type 2 diabetes and stage 4 chronic kidney disease. N Engl J Med 369: 2492–2503.

Zhang S, Leske DA, Holmes JM (2000). Neovascularization grading methods in a rat model of retinopathy of prematurity. Invest Ophthalmol Vis Sci 41: 887–891.

Zhong Q, Mishra M, Kowluru RA (2013). Transcription factor Nrf2-mediated antioxidant defense system in the development of diabetic retinopathy. Invest Ophthalmol Vis Sci 54: 3941–3948.